2015 IEEE/RSJ International Conference on Intelligent Robots and Systems (IROS)
Congress Center Hamburg
Sept 28 - Oct 2, 2015. Hamburg, Germany

Monolithic Fabrication of Sensors and Actuators in a Soft Robotic Gripper

R. Adam Bilodeau[1], Edward L. White[1] and Rebecca K. Kramer[1*]

***Abstract*— In this paper, we present a fluidically functionalized soft-bodied robot that integrates both sensing and actuation. Rather than combining these functions as an afterthought, we design sensors and actuators into the robot at the onset, both reducing fabrication complexity and optimizing component interactions. We utilize liquid metal strain sensors and pneumatic actuators embedded into a silicone robotic gripper. The robot's body is formed by curing the silicone in complex 3D printed molds. We show that the liquid metal strain gauges provide a repeatable resistance response during robotic actuation. We further show that, given sufficient control over other time-dependent variables, it is possible to determine when the robot begins gripping an object during actuation.**

I. Introduction

Researchers in robotics are beginning to diverge from the traditional rigid robots that are so prominent in manufacturing. Engineers in the emerging field of soft robotics are working on solving problems that cannot be solved easily with rigid robots, including improving human-robot interactions, developing formable robots that can adapt to varying geometric constraints, and robots that can absorb impacts/shocks by deforming their main body. Silicone-bodied pneumatic robots have helped to shape the idea of a truly "soft" robot, since most of the body is formed out of a soft, elastomeric material with an extremely low stiffness [1]. Many of the silicone elastomers used in soft robotics are capable of sustaining strains anywhere from 100-500% [2]. Since these elastomers are highly deformable, engineers can inflate internal pneumatic channels to provide rigidity and stability to the robot. With the proper configuration, such robots can use their pneumatically actuated components to gain form, function, and even locomotion [1], [2], [3].

One of the challenges associated with soft robotic design is adding sensors that can close the robotic control loop. Researchers are actively working on soft-bodied control methods [4], [5], [6], but lack general proprioceptive feedback sensors for soft robots. Since soft robots undergo extremely high strains during actuation, traditional feedback systems either break or are difficult to attach to the robot. One solution to high deformation strain sensing has been to create a strain gauge made out of a room-temperature liquid metal embedded in an elastomeric matrix [7], [8]. These strain gauges can be an effective way of gathering data in some robots [9], but the issue of attaching the gauges to the robot remains an open problem.

*Author to whom correspondence should be addressed rebeccakramer@purdue.edu
[1]Department of Mechanical Engineering, Purdue University, West Lafayette, IN 47907, USA

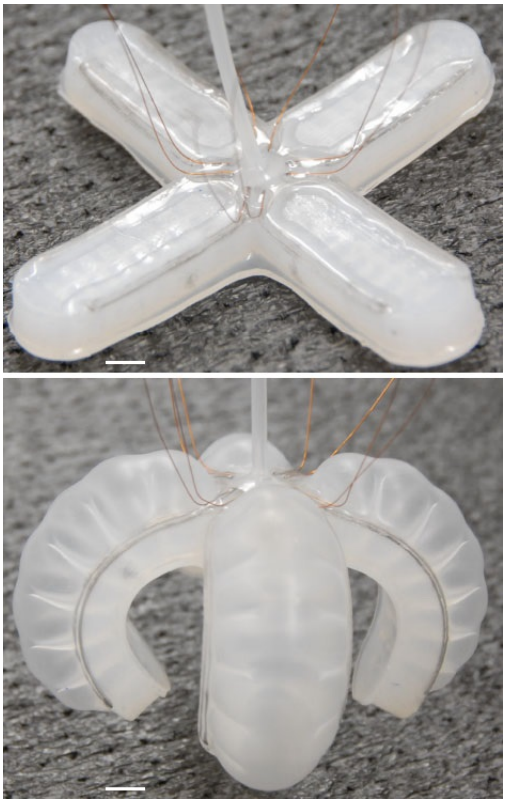

Fig. 1. Pneumatic robot with liquid metal sensors embedded into the body. Above: the robot in its relaxed state. Below: the robot after pneumatic actuation. Scale bars are 1 cm.

In this paper, we present a manufacturing process that incorporates liquid metal strain sensors directly into the body of a 4-arm, pneumatically-actuated, soft robotic gripper (see Figure 1). This is in contrast to previous work where the sensors and actuators are built separately and integrated afterwards. In the robot, each strain sensor is independent of the others and capable of providing real-time feedback about the actuation of the arm of the robot. The feedback from the sensors can be characterized in a way that distinguishes activated states of the robotic gripper and, given control over other actuation parameters, makes it possible to determine if the robot is gripping an object or not.

II. Previous Work

A pneumatically-actuated soft robot was described in detail by Shepherd, et al. [1]. This robot was actuated through pressurization of internal cavities called "pneu-nets" formed within a highly elastic polymer body. This work has been extended by researchers who have all primarily focused

on improving actuation. Great strides have been made in improving the speed of pneumatic actuation [2], [10] and in untethering pneumatic robots from an external compressed air source [3], [4]. Other researchers have created soft-hard hybrids that take advantage of the strengths associated with both rigid robots and soft pneumatically-actuated robots to perform tasks that neither can do alone [11].

Sensors for soft robotic systems have also been an area of recent research, as they provide state reconstruction that allows for control feedback. One approach to sensing in soft-bodied systems is with eutectic gallium indium alloy (eGaIn) encased in microchannels within a highly elastic substrate. Gallium indium alloy is a room-temperature liquid metal that is non-toxic and highly conductive [12], [13]. The basic principle behind these high displacement strain gauges is simple: as the elastomer is stretched, the length of the channel increases and the cross-sectional area is reduced. Changing the geometry of the channel alters the resistance across the channel (following basic resistance laws), providing sensory feedback on the physical deformation. Since the conductor inside of the channel is liquid, and the matrix surrounding it is highly elastic, the gauges are ideal for large strain applications. Park, et al. investigated the sensitivity of this class of devices to variations in channel geometry [14].

Gallium indium alloy has been used in a number of different soft robotic applications. Examples of sensing elements fabricated from eGaIn-filled microchannels include curvature sensors [15], [16], stress sensors [17], [18], and strain sensors [19], [20]. The sensors we have fabricated into our robot rely on the same mechanism as those previously discussed. What is unique about our approach is that the sensor is fabricated directly into the robot instead of as a separate structure.

III. Experimental

A. Fabrication

The initial pattern for the pneumatic robot is a derivative of a simplified pneumatic robot designed by Finio et al. [21]. We started with this concept because it is extremely simple, and allowed us to focus on adding sensory elements to the robot instead of focusing on the pneumatic robot body design. The robot is a composite of two silicones: Ecoflex 00-30 (Smooth-On, with hardness below the Shore A scale) to form the pneumatic channels and the main body, and Silgard 184 (PDMS, DowCorning, Shore A hardness of 50) to seal the channels. The design has a single air input port and is formed with a 3D printed mold. We kept the single fill port design as it allowed us to simultaneously activate and control all arms of the robot from the same air source, but we modified the fabrication method so that we could incorporate sensory channels into the robot. Because the molds were simple and easy to form in a 3D printer, we were able to quickly iterate though different methods to integrate the sensors.

Our modified process includes a 2-step mold (Figure 2) for the main body that embeds the pneumatic channels and the sensory channels into the Ecoflex body. As demonstrated in Figure 3a-3d, we first filled the primary mold (depicted in Figure 2a) with uncured Ecoflex. This section of the mold has embossed features to create channels for the liquid metal sensors. The mold for the pneumatic channels (depicted in Figure 2b) was then lowered into the Ecoflex, creating hollows on the opposite side of the robot body from the liquid metal sensor channels. The Ecoflex was allowed to cure completely and was removed from the mold.

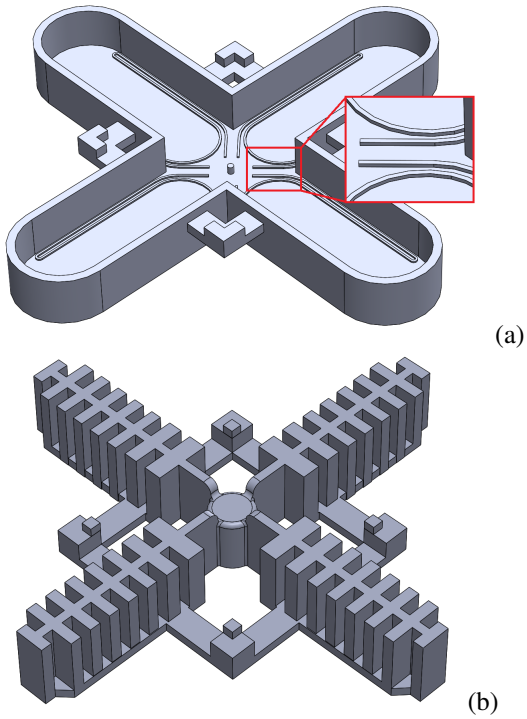

Fig. 2. 3D modeling representations of the molds that were printed to cast the robot. (a) The primary mold, initially filled with liquid elastomer, with an inset showing the embossed channels that create the sensor channels. (b) The channel mold that is placed in the primary mold to create the pneumatic channels in the robot.

Figures 3e-3f show the next two steps of the process. We filled the open serpentine channels with room temperature liquid metal (eGaIn, Sigma-Aldrich). Once the channels were filled, a small amount of liquid Ecoflex was placed over the channels to seal them. Most soft strain sensors are sealed before being filled with liquid metal [19], but in our case we found that it was easier to seal them afterward. When sealing the channels, we took care to prevent the liquid elastomer from running across the top of the robot and building up a thick layer of polymer. Because the curling actuation motion is a result of the stiffness difference between the bottom and the top of the robot, both material properties and geometric design can change the stiffness and therefore change the actuation motion. A thicker layer of Ecoflex on top of the robot would increase stiffness and result in less curl in the robotic arm. Once the silicone cured, we punctured the thin layer with the electrical wiring, making a contact with the liquid metal. The wires were then folded down and sealed onto the robot with a few more drops of liquid elastomer, preventing the wires from pulling out while the robot is undergoing large deflections. The pneumatic tube was also

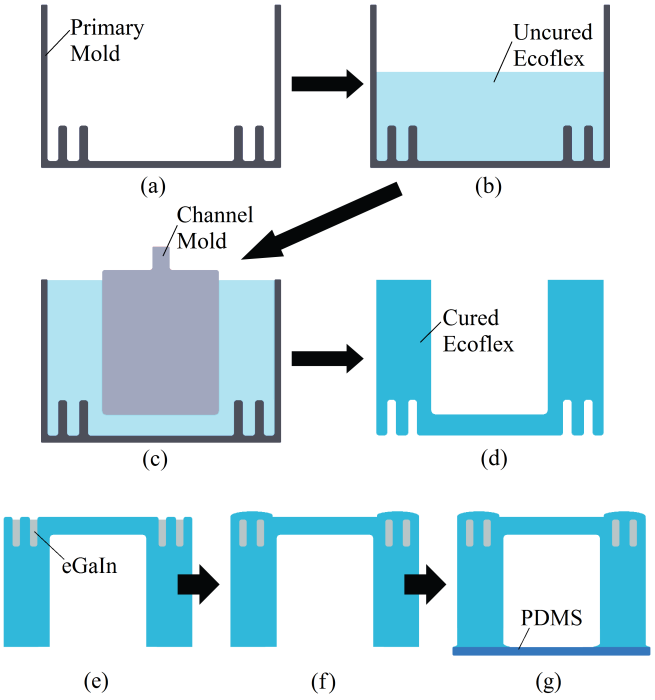

Fig. 3. (a) The bottom half of the mold is printed and (b) filled with liquid elastomer. (c) The channel mold (previously printed) is embedded inside the liquid elastomer to create the pneumatic channels. When the elastomer has cured (d) the mold can be removed from around it. To finish the sensors, (e) the eGaIn channels are filled with liquid metal and (f) sealed with liquid elastomer. Finally, (g) the pneumatic channels are sealed by bonding the body to a thin layer of Silgard 184.

punctured into the robot through a central hollow (created in the mold) and sealed in the same manner. To finish building the pneu-nets, we prepared and cured a thin, flat layer of Silgard 184. We then sealed the two layers together by adding a small amount of liquid elastomer on top of the Silgard 184 and placing the body of the robot down onto the layer. When the liquid elastomer cured, it bonded the two halves of the robot together (Figure 3g).

B. Sensor Design

Our initial, unsuccessful, sensor design placed the sensors down the center of the pneumatic arm, the area that experiences the greatest strain during actuation. Although we did this to maximize the response from the gauges, the strain gauges would either lose conductivity or break completely. Loss of conductivity occurred during inflation, when the outside of the pneu-nets experienced biaxial strains (along the length and width of the robotic arm). These strains induced channel collapse, forcing the eGaIn to withdraw from sections of the channel and breaking conductivity (see Figure 4). After actuation, the channel would need to be massaged to push the eGaIn back into the pinched area, removing any potential automation from this design. Furthermore, the channels did not have a high fatigue life. Previous demonstrations have shown the silicone in these types of pneumatic robots will endure many cycles of actuation without failure [1], [10]. However, when we placed the

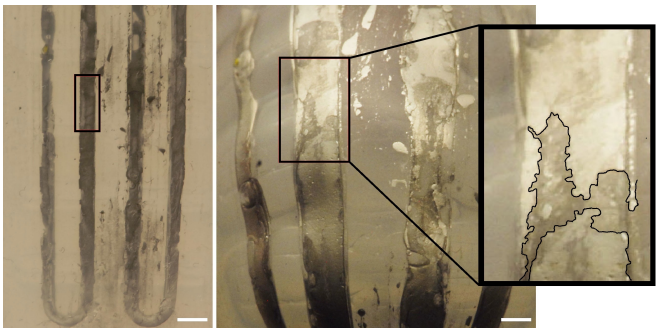

Fig. 4. A preliminary design with the liquid metal sensors directly over the pneumatic channels. The image on the left is the top of the channels before the arm is inflated (the surface is flat), and the image on the right is the same surface, at the same scale, after it is inflated. The liquid metal channels undergo a large increase in both length and width causing an extreme collapse in the channel's third dimension. The box in both photos is surrounding the same section of the sensor. The inset is a magnification of the inflated channel with an outlined area that experienced eGaIn withdrawl due to the channel collapse. The scale bars on both images are 2mm, and the inset has 2.5x magnification.

sensors over the areas of highest strain, the silicone (Ecoflex) sealing the liquid-metal channels was unable to sustain the repeated strains and the sensors would burst after 5-10 cycles. Adding a thicker layer of elastomer mitigated this issue, but it did so by significantly impacting the actuation dynamics of the robot.

We studied the robot during actuation to find a location for the sensors that could result in appropriate dynamic response without failure. Pneumatic channels are typically designed with regions that have a thicker cross section than other locations (see Figure 3). This helps create a specific motion in the arm during pneumatic actuation [2]. Although these sections deform, they are not subjected to the same magnitude of strains as the original location we selected for the sensors. In the final design of our robot, we embedded the serpentine liquid metal pattern into these sections (see Figures 3 and 5), preventing many of the problems associated with previous design locations. Furthermore, finite element analysis by Mosadegh et al. suggests that our selected location still experiences moderate strains and stresses during actuation [10]. Though we do not claim that this location is perfectly optimized, identifying a location that experiences strain, but is not excessively stressed, is key to successfully integrating feedback strain sensors directly into the bodies of soft robots.

C. Sensor Characterization

Our sensor characterization tests were designed to provide evidence of the success of our proof-of-concept robot. We performed a simple test on one of the robot's arms to ensure that the strain gauge location provides a measurable response during actuation. We measured the sensor's response to two different modes of strain: linear extension and pneumatic actuation (Figure 6). For the linear extension tests, we pulled the tip of the robot arm linearly away from the body of the robot, duplicating a load similar to that of a normal strain gauge [22]. We then used a hand pump to pneumatically

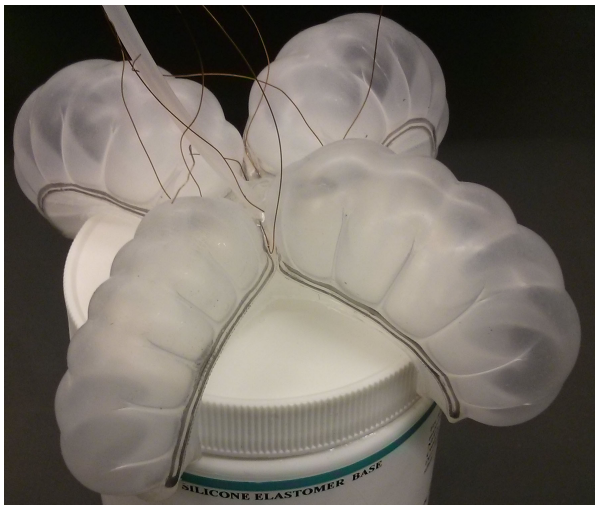

Fig. 5. The pneumatic robot gripping a cylindrical container. The serpentine liquid-metal sensor channels are clearly visible around the outside edges of the pneumatic channels (dark against the white background).

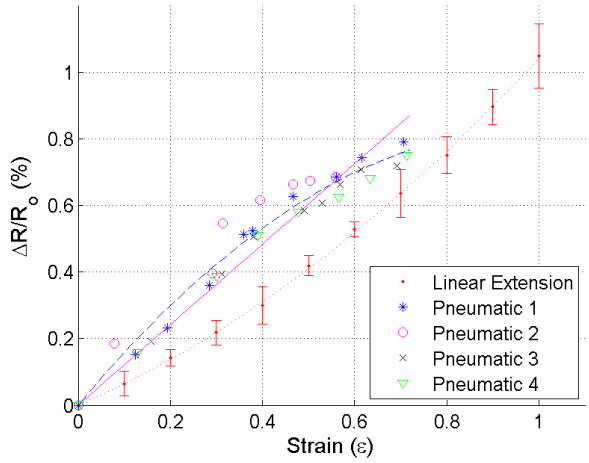

Fig. 6. A comparison of the strain gauge's percent increase in resistance for one of the robot arms experiencing two modes of strain. The linear extension tests were an application of unidirectional strain to the arm. The error bars are a 90% confidence interval, and the red dotted line is a fit of the data. The other four tests were performed by pneumatically actuating the robot and recording the resistance change, with the solid magenta line representing a linear fit and the blue dashed line representing a curved fit of all the tests.

actuate the robot in steps while taking profile photographs of the arm, which we analyzed to measure the length change of the liquid metal sensors.

D. Sensor-Actuator Interaction

To test the robot's potential for automated control, we measured the resistance of the strain sensors in each arm in real time while actuating the robot using a constant air flow. To measure the resistance in the gauges, we wired each sensor as a resistor in a voltage dividing circuit. Because of the low resistivity of eGaIn ($\sim 29.4 \times 10^{-6}\Omega$-cm [23]), a small 2 Ohm resistor was added as the second resistor in each circuit. Using a KORAD KA3005D DC power supply we limited the voltage across the whole system to 0.7V to prevent excessive current draw through the low resistance devices. To activate the robot, we attached it to a compressed air source with a flow-valve control system that limited the gauge pressure to between 5 and 6 KPa during the tests. We chose a low air pressure for the input line to limit the air flow velocity and slow the actuation of the robot to the timescale of the test. During actuation, we measured the voltage across the strain gauges using a Tektronics TDS 2014C 4-channel input oscilloscope limited to a 50 Hz measuring frequency. Although the oscilloscope had 4 channels for input, one of the channels was dedicated to measuring the voltage across an electronic gauge-pressure sensor (Honeywell 001PDAA5, DigiKey), which provided a digital marker that was used to synchronize the different tests. This limited us to characterizing only three of the four arms, which were picked at random from the robot.

At the beginning of each test we recorded the initial resistance for several seconds with the robot in its resting state. Each characterization test then consisted of filling the robot with air for 5 seconds while measuring the voltage drop across the arms, and releasing the air in the robot. After the robot returned to its resting state, we recorded another brief dwell period before actuating the robot again. We tested the robot actuating under two test conditions: the robot actuating in empty air (see Figure 1) and the robot clamping a cylindrical object (see Figure 5) with a radius of about 4.5cm. We filmed each test so that we could compare the recorded data to events that the robot was experiencing.

The pressure sensor was connected to the robot's input valve, and indicated when the pressure in the infill tube changed. There was a nearly instantaneous change after the valve was opened, and the pressure remained constant during the tests. The recorded initial pressure spike acted as a time marker, enabling us to overlay all the tests we ran on the robot under both testing conditions.

IV. Results and Discussion

Change in resistance as a function of strain for two loading conditions is shown in Figure 6. Engineering strain was calculated from the extended length of the strain gauge. In the case of the linear extension tests, this was measured during the test. The extended length of the strain gauge during pneumatic actuation was considered to be the arc-length of the gauge, as seen from a profile view. The percent change in resistance was calculated by dividing the actuated resistance by the initial resistance.

These tests demonstrate our success in integrating the sensors into the robot's body. Figure 6 shows that the strain gauges are appropriately placed and return results that correlate strain to a resistance change. There is a high degree of repeatability in the results from both the uniaxial tests and the pneumatic actuation tests. The curve fit to the linear extension data is characteristic of uniaxial strain gauges and agrees with the literature [20], [24], [25], [26]. The pneumatic actuation data also increases monotonically,

however, it does not display the quadratic response typical of uniaxial strain loading. For clarity, we have included two possible fits to the data: a linear fit and an inverse quadratic fit. We note that a more in-depth model and expanded data range would be needed to verify either trend. Nonetheless, the pneumatic actuation data has sufficient contrast from the linear extension data to indicate that the strain gauges undergo a complex strain state that is not purely uniaxial during actuation.

To analyze the data gathered during the gripping actuation tests, we first applied a 20 point moving average filter to remove the noise. We then used basic electrical circuit theory to calculate the resistance in each strain gauge based on the measured voltage. We noticed that each of the robot's arms had a different initial resistance and electrical response to actuation. To permit easy comparison between the three different arms, we calculated the percentage rise of resistance based off of the total overall change that the sensor underwent when gripping the cylinder. We present the results of our 3 tests with a 90% confidence interval in Figure 7. Though a 50 Hz signal with a 20 point filter slows down the response time of a control system, the inherently high compliance in the soft robot tolerates imprecision in the control while preventing damage to the robot or the object being gripped, ideally simplifying feedback control.

Each arm's strain gauge demonstrates a similar response during the tests. When gripping air, there is a consistent increase in resistance throughout the whole test. During the object gripping tests, each sensor initially experiences the same increase as the control, with a sudden departure from the trend when the robot begins to contact and grip the object. The videos of the tests validate that at about 3s the robot begins to contact and grip the object, matching the recorded data (Figure 7). By keeping the inflow pressure controlled, the strain gauges provide feedback in a predictably linear manner until boundary conditions change (an object is encountered). Since the slopes of each section of the data are constant, it is possible to distinguish the time that the robot begins to grip an object. This performance is consistent with the observations performed by Kramer et al. with their liquid metal curvature sensors. By changing the boundary conditions of their curvature sensors (from air to a rigid joint), they experienced a magnification of the resistance change by over an order of magnitude [16]. This means that the integrated strain gauges can be used to mark events (such as gripping or other boundary changes) during the actuation of the robot.

V. Conclusion

We prototyped a pneumatically actuated soft robot with liquid metal strain gauges built into the soft robot's body that provide real-time feedback during actuation of the robotic system. Two simple tests on the robot provided strong evidence of the validity of this integrated sensor design. Under controlled conditions, the resistance in the strain gauges changes in a predictable manner relating directly to both the strain in the robot's arms and the rate of actuation.

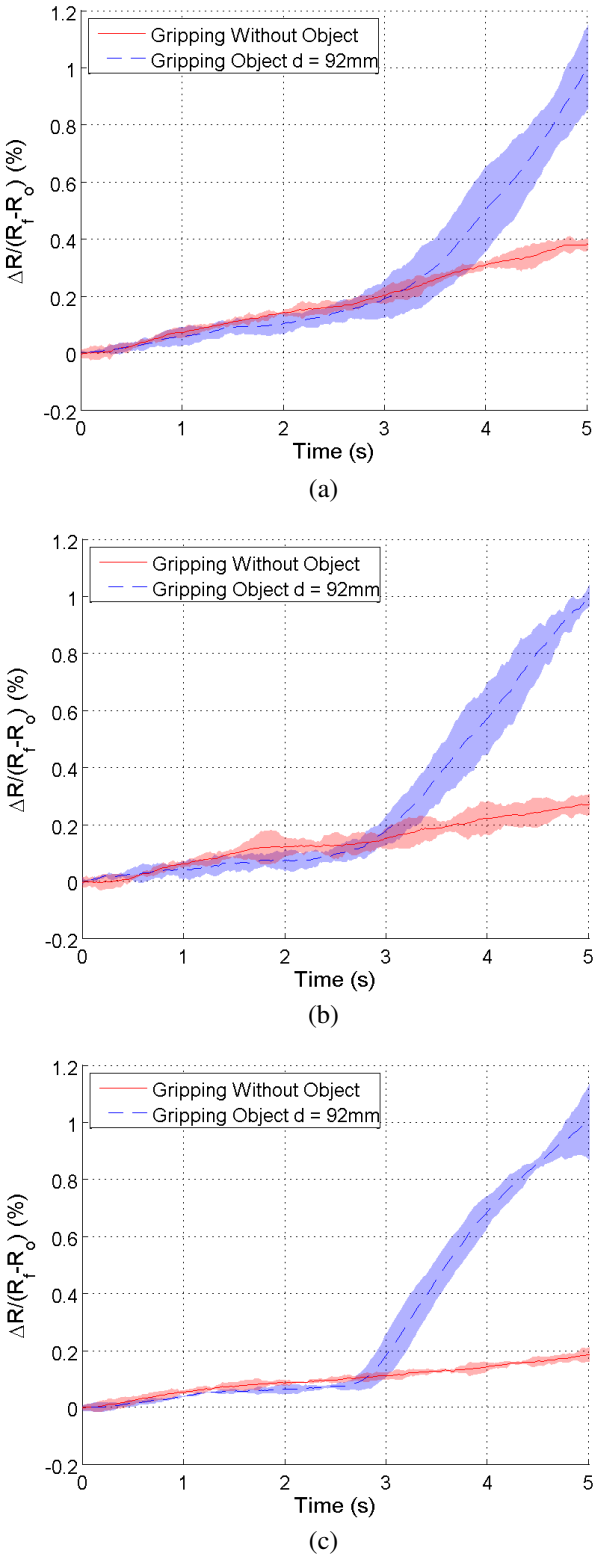

Fig. 7. The resistance change in three of the robot's strain sensors during the 5s actuation tests. Each graph (a,b,c) represents a different arm on the robot. The test setup only permitted gathering simultaneous data from 3 arms, though the sensors on all 4 arms were fully functional. The solid red line is the average of the baseline tests (the robot inflating in empty air). The dashed blue line is the average of the tests with the robot gripping the test cylinder at approximately 3 seconds. The shaded area surrounding each line represents a 90% confidence interval. The percent change was calculated using the initial and final resistances of the tests with the robot gripping an object.

We also show that, under a constant input air pressure, we can sense if and when the robot is gripping an object. The modified fabrication method of these robots is outlined so that this work can be easily expanded on in the future.

VI. Future Work

This proof of concept robot demonstrates significant potential for many future projects that integrate sensors into the body of a pneumatically actuated robot. It has the possibility of finally closing the control loop and opens up a greater potential to automate soft robots. Each sensors' response to actuation can be characterized independently, eventually allowing for computer control to optimize the actuation in each arm. Furthermore, since each arm provides actuation and gripping feedback independently of the other arms, there is redundancy in the gripping information provided to the robotic controller. Regardless of the complexity of the eventual model, the repeatability of our simple tests demonstrate the potential to use the resistance response in the gauge to generate a state reconstruction model for control of a pneumatic robot.

We also believe that there are more possibilities for sensor locations and types on a pneumatic robot like that presented in this paper. In the future, we would like to integrate pressure sensors into the Silgard 184 bottom layer of the robot (which is the side that grips objects). This will provide a secondary sensory system that a computer controller can use to determine if an object is being gripped and potentially how much force is being applied to grip an object. These sensors may also be able to provide a faster feedback response to a control system than our currently heavily filtered system. This would free up the strain sensors to be primarily used for arm position and location control.

VII. Acknowledgments

ELW is supported under the National Science Foundation Graduate Research Fellowship program (DGE-1333468). Any opinions, findings, and conclusions or recommendations expressed in this material are those of the author and do not necessarily reflect the views of the National Science Foundation.

References

[1] Robert F. Shepherd, Filip Ilievski, Wonjae Choi, Stephen A. Morin, Adam A. Stokes, Aaron D. Mazzeo, Xin Chen, Michael Wang, and George M. Whitesides. Multigait soft robot. 108(51):20400–20403.

[2] Filip Ilievski, Aaron D. Mazzeo, Robert F. Shepherd, Xin Chen, and George M. Whitesides. Soft robotics for chemists. 50(8):1890–1895.

[3] Michael T. Tolley, Robert F. Shepherd, Bobak Mosadegh, Kevin C. Galloway, Michael Wehner, Michael Karpelson, Robert J. Wood, and George M. Whitesides. A resilient, untethered soft robot. 1(3):213–223.

[4] Cagdas D. Onal, Xin Chen, George M. Whitesides, and Daniela Rus. Soft mobile robots with on-board chemical pressure generation. In *International Symposium on Robotics Research*, pages 1–16.

[5] Sangok Seok, C.D. Onal, Robert Wood, D. Rus, and S. Kim. Peristaltic locomotion with antagonistic actuators in soft robotics. In *2010 IEEE International Conference on Robotics and Automation (ICRA)*, pages 1228–1233.

[6] Cagdas D. Onal and Daniela Rus. Autonomous undulatory serpentine locomotion utilizing body dynamics of a fluidic soft robot. 8(2):026003.

[7] John A. Rogers, Takao Someya, and Yonggang Huang. Materials and mechanics for stretchable electronics. 327(5973):1603–1607.

[8] Michael D. Dickey. Emerging applications of liquid metals featuring surface oxides. 6(21):18369–18379.

[9] M. Yuen, A. Cherian, J.C. Case, J. Seipel, and R.K. Kramer. Conformable actuation and sensing with robotic fabric. In *2014 IEEE/RSJ International Conference on Intelligent Robots and Systems (IROS 2014)*, pages 580–586.

[10] Bobak Mosadegh, Panagiotis Polygerinos, Christoph Keplinger, Sophia Wennstedt, Robert F. Shepherd, Unmukt Gupta, Jongmin Shim, Katia Bertoldi, Conor J. Walsh, and George M. Whitesides. Pneumatic networks for soft robotics that actuate rapidly. 24(15):2163–2170.

[11] Adam A. Stokes, Robert F. Shepherd, Stephen A. Morin, Filip Ilievski, and George M. Whitesides. A hybrid combining hard and soft robots. 1(1):70–74.

[12] Michael D. Dickey, Ryan C. Chiechi, Ryan J. Larsen, Emily A. Weiss, David A. Weitz, and George M. Whitesides. Eutectic gallium-indium (EGaIn): A liquid metal alloy for the formation of stable structures in microchannels at room temperature. 18(7):1097–1104.

[13] Ryan C. Chiechi, Emily A. Weiss, Michael D. Dickey, and George M. Whitesides. Eutectic galliumindium (EGaIn): A moldable liquid metal for electrical characterization of self-assembled monolayers. 120(1):148–150.

[14] Yong-Lae Park, Daniel Tepayotl-Ramirez, Robert J. Wood, and Carmel Majidi. Influence of cross-sectional geometry on the sensitivity and hysteresis of liquid-phase electronic pressure sensors. 101(19):191904.

[15] C. Majidi, R. Kramer, and R. J. Wood. A non-differential elastomer curvature sensor for softer-than-skin electronics. 20(10):105017.

[16] R.K. Kramer, C. Majidi, R. Sahai, and R.J. Wood. Soft curvature sensors for joint angle proprioception. In *2011 IEEE/RSJ International Conference on Intelligent Robots and Systems (IROS)*, pages 1919–1926.

[17] Yong-Lae Park and R.J. Wood. Smart pneumatic artificial muscle actuator with embedded microfluidic sensing. In *2013 IEEE Sensors*, pages 1–4.

[18] Yong-Lae Park, Bor-Rong Chen, and Robert J. Wood. Design and fabrication of soft artificial skin using embedded microchannels and liquid conductors. 12(8):2711–2718.

[19] J.-B. Chossat, Yong-Lae Park, R.J. Wood, and V. Duchaine. A soft strain sensor based on ionic and metal liquids. 13(9):3405–3414.

[20] J. William Boley, Edward L. White, George T.-C. Chiu, and Rebecca K. Kramer. Direct Writing of Gallium-Indium Alloy for Stretchable Electronics. *Advanced Functional Materials*, 24(23):3501–3507, June 2014.

[21] Benjamin Finio, Robert Shepherd, and Hod Lipson. Air-powered soft robots for k-12 classrooms. In *Proceedings of the IEEE Integrated STEM Education Conf.(ISEC)*, pages 1–6.

[22] Jennifer C. Case, Edward L. White, and Rebecca K. Kramer. Soft Material Characterization for Robotic Applications. *Soft Robotics*, 2(2):80–87, June 2015.

[23] D. Zrnic and D. S. Swatik. On the resistivity and surface tension of the eutectic alloy of gallium and indium. 18(1):67–68.

[24] Hyun-Joong Kim, T. Maleki, Pinghung Wei, and B. Ziaie. A biaxial stretchable interconnect with liquid-alloy-covered joints on elastomeric substrate. 18(1):138–146.

[25] Shu Zhu, Ju-Hee So, Robin Mays, Sharvil Desai, William R. Barnes, Behnam Pourdeyhimi, and Michael D. Dickey. Ultrastretchable fibers with metallic conductivity using a liquid metal alloy core. 23(18):2308–2314.

[26] Johannes T. B. Overvelde, Yiit Meng, Panagiotis Polygerinos, Yunjie Wang, Zheng Wang, Conor J. Walsh, Robert J. Wood, and Katia Bertoldi. Numerical mechanical and electrical analysis of soft liquid-embedded deformation sensors. *Extreme Mechanics Letters*, 2014.